



## Article

# Selective Flotation of Pyrite from Galena Using Chitosan with Different Molecular Weights

Wanjia Zhang <sup>1,2</sup> , Wei Sun <sup>1,2</sup>, Yuehua Hu <sup>1,2</sup>, Jian Cao <sup>1,2,3,4,\*</sup> and Zhiyong Gao <sup>1,2,\*</sup> <sup>1</sup> School of Minerals Processing and Bioengineering, Central South University, Changsha 410083, China<sup>2</sup> Key Laboratory of Hunan Province for Clean and Efficient Utilization of Strategic Calcium-Containing Mineral Resources, Central South University, Changsha 410083, China<sup>3</sup> Guangdong Institute of Resources Comprehensive Utilization, Guangzhou 510651, China<sup>4</sup> Guangdong Provincial Key Laboratory of Development and Comprehensive Utilization of Mineral Resources, Guangzhou 510651, China

\* Correspondence: caojianlzu@163.com (J.C.); zhiyong.gao@csu.edu.cn (Z.G.); Tel.: +86-198-0749-8656 (J.C.); +86-135-7489-2751 (Z.G.)

Received: 29 July 2019; Accepted: 6 September 2019; Published: 12 September 2019



**Abstract:** Pyrite is a major gangue mineral associated with galena and other valuable minerals, and it is necessary to selectively remove pyrite to upgrade the lead concentrate by froth flotation. In this study, the flotation experiments of a single mineral and mixed minerals were performed using chitosan with different molecular weights (MW = 2–3, 3–6, 10 and 100 kDa) as a depressant, ethyl xanthate as a collector, and terpeneol as a frother, in a bid to testify the separation of pyrite from galena. Flotation results showed that the selective flotation of pyrite from galena can be achieved under the preferred reagent scheme, i.e., 400 g/t chitosan (10 kDa), 1600 g/t ethyl xanthate, and 100 g/t terpeneol, while chitosan with other molecular weights cannot. Furthermore, the results of the zeta potential and contact angle measurements revealed that chitosan (10 kDa) has a strong adsorption on galena yet a very weak adsorption on pyrite at the dosage of 400 g/t. This study showed that chitosan (10 kDa) has great potential in the industrial flotation separation of pyrite from lead concentrates.

**Keywords:** chitosan; molecular weight; selective depression; reverse flotation; pyrite; galena

## 1. Introduction

Pyrite (FeS<sub>2</sub>) is the main gangue associated with valuable sulfide ores, such as galena, chalcopyrite, sphalerite, and others [1–5]. Pyrite is usually depressed during the flotation of sulfide minerals [6] by the use of a depressant [4,7], pulp-environment management [8,9], and grinding-environment changes [10,11]. Although these techniques were proven to be effective, the loss of valuable minerals in tailings [12,13] and the doping of pyrite in concentrates [14] still cannot be ignored.

According to the principle of “float less and depress more”, it is more cost-effective to reversely float pyrite while depressing lead concentrates, in a bid to upgrade lead concentrates containing pyrite impurities [15]. Our previous studies have also confirmed that reverse flotation is an effective method to improve the grade of desired mineral/metal in flotation concentrate, and the development of a new reagents scheme [16–18] is the key to achieve this [19,20]. Therefore, in this study, we explored an efficient and highly selective galena depressant and a pyrite-removal strategy to upgrade lead concentrates.

Polysaccharide polymers [21–24] are a hot topic in mineral processing due to their efficiency and degradability as the depressants for the flotation of sulfide ores [25–27]. In recent years, there were many reports on the relations between the depression effect of macromolecular depressants and molecular weight (MW), i.e., low molecular weight (LMW: 1 kDa ≤ MW < 50 kDa), medium molecular weight (MMW: 50 kDa ≤ MW < 500 kDa), and high molecular weight (HMW: 500 kDa ≤ MW < 1000 kDa) [28–31]. These studies

showed that MMW-macromolecule depressants can selectively depress the mixed-mineral systems through competitive adsorption. However, the selective depression effect of MMW-macromolecule depressants is still not satisfactory, especially for polymetallic sulfide ores.

In this study, the depression effect of chitosan with different molecular weights (ULMW (ultralow molecular weight) = 2–3, 3–6 kDa, LMW = 10 kDa, and MMW = 100 kDa) on galena and pyrite were investigated, and a novel reagent mode was used to evaluate the flotation behavior of the single mineral. The separation performance of this novel reagent mode was testified by the mixed-mineral flotation experiments, and the mechanism of the selective separation was investigated through zeta potential measurements and contact angle tests.

## 2. Materials and Methods

### 2.1. Materials and Reagents

The pure pyrite and galena crystal samples were obtained from the Huangshaping Mine, Hunan, China. Firstly, the commonly exposed cleavage surfaces were carefully selected and cleaved to collect samples for contact angle tests. The selected pyrite and galena crystals were respectively embedded in the resin, and the required surfaces remained exposed for further grinding and polishing. In a bid to obtain a flat surface, the desired exposed surfaces of pyrite and galena were successively ground by sandpapers at a roughness of 90, 38, 18, 6.5, and 2.5  $\mu\text{m}$ . The ground surfaces were successively polished with an alumina powder (1.0, 0.5, and 0.05  $\mu\text{m}$ ) solution on a polishing cloth [32].

Pure pyrite and galena crystal samples were freshly ground in a ceramic ball mill (Tencan Powder Co., Ltd., Changsha, China) and screened for required flotation samples with a size of  $-74 + 37 \mu\text{m}$ . Samples stored within 1–3 days after preparation were further ground to  $-5 \mu\text{m}$  in an agate mortar and used for X-ray powder diffraction and zeta potential measurements. As shown in Figure 1, the X-ray powder diffraction spectra of the pyrite and galena samples confirmed that both the pyrite and galena samples were sufficiently pure.

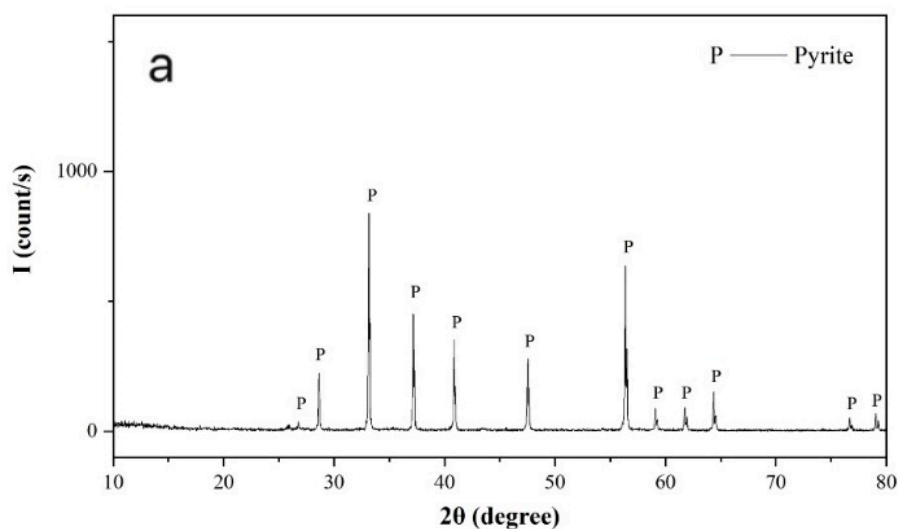
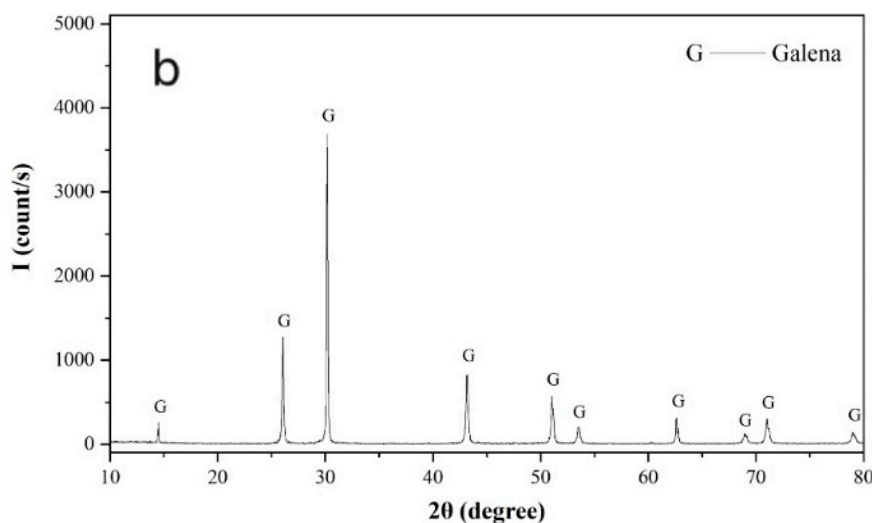


Figure 1. Cont.



**Figure 1.** XRD spectrums of (a) pyrite and (b) galena particle samples.

The ethyl xanthate (90%, Macklin Chemical Reagent Co., Ltd., Changsha, China) was used as a collector [33], the terpeneol (90%, Tianjin Kermil Chemical Reagent Centre, Tianjin, China) as a frother [34], and the chitosan (Bomei Biotechnology Co., Ltd., Hefei, China) (2–3, 3–6, 10 and 100 kDa, chitosan >99%, water-soluble, deacetylation rate >85%) as depressants. The colors and morphologies of chitosan with different molecular weights are shown in Figure 2, and the structural unit of chitosan is shown in Figure 3. When the pulp pH was not equal to 8, the pulp condition was adjusted with HCl and NaOH stock solutions (0.1 mol/L). All experiments were carried out in deionized (DI) water with a resistivity of over  $18 \text{ M}\Omega \times \text{cm}$ .



**Figure 2.** The morphologies of chitosan with different molecular weights: (a) 2–3 kDa chitosan; (b) 3–6 kDa chitosan; (c) 10 kDa chitosan; (d) 100 kDa chitosan.

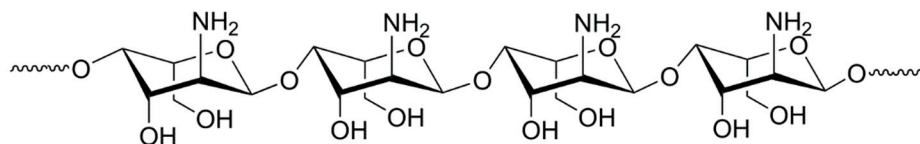


**Figure 3.** The structural unit of chitosan.

## 2.2. Flotation Experiments of Single Mineral and Mixed Minerals

The flotation experiments were carried out in an XFG-type flotation machine [19,35–38] at a spindle speed of 1850 rpm. In each flotation experiment, a single-mineral sample (2.00 g) or mixed-mineral sample (1.00 g pyrite plus 1.00 g galena) was added to the flotation cell (with 40 mL DI water) to obtain the mineral suspension. If necessary, HCl or NaOH stock solution (0.1 mol/L) was added to adjust the pulp pH. Then, chitosan (2–3, 3–6, 10, and 100 kDa), ethyl xanthate, and terpeneol with the desired dosage were added in sequence, and floated products were collected for 3 min. Finally, the flotation concentrates and tailings were filtered, dried, and weighed for recovery calculation. At the same time,

Fe and Pb grades of flotation concentrates and tailings were assayed. Each flotation experiment was repeated three times to obtain an average value.

### 2.3. Zeta Potential Measurements

The zeta potential measurement is a common electrochemical test used to detect the reaction process on mineral surfaces and adsorption behavior of flotation reagents [39]. Zeta potential measurements were conducted at 20 °C, using a Zetasizer Nano series (Malvern, United Kingdom). The mineral suspension was prepared by adding a pyrite or galena sample (20 mg,  $-5\ \mu\text{m}$ ) to a KCl electrolyte solution (0.01 mol/L, 40 mL) in a beaker (100 mL), at a given pH value and chitosan dosage. The mineral suspension was then used for zeta potential measurements after magnetically stirring for 15 min and standing for 5 min. Each zeta potential was tested six times, and the average value was obtained.

### 2.4. Contact Angle Tests

The contact angle test is a common method to detect the hydrophobic changes of mineral surfaces in the presence or absence of flotation reagents [40]. The wettability of the prepared pyrite and galena samples in the presence or absence of chitosan with different molecular weights at a dosage of 400 g/t was measured at pH 8. The prepared pyrite or galena sample was first immersed in a beaker (150 mL) containing a given solution (100 mL) and stirred at 20 °C for 30 min. Then, the sample was taken out, gently washed with DI water, and vacuum dried at 50 °C for 10 min, followed by measuring contact angles via the water droplet method [41]. In each contact angle test, droplets of 3.5  $\mu\text{L}$  DI water were added, and 25–35 s later, when a stable state was reached, the contact angles were calculated based on the shape of the droplets (Windrop++ Software). Under each condition, contact angle tests were carried out three times, to take the average value. After each test, the sample surface was repeatedly washed with DI water and alcohol. Finally, the sample was polished using a 0.05  $\mu\text{m}$  alumina powder solution for the next test.

## 3. Results

### 3.1. Single-Mineral Flotation Experiments Results

Using different molecular weights of chitosan as depressants, ethyl xanthate as a collector, and terpineol as a frother, the flotation behavior of pyrite and galena was evaluated by the single-mineral flotation, with results shown in Figure 4. At a certain dosage, with the increase of the chitosan molecular weight, the flotation recoveries of pyrite and galena decrease gradually. The flotation recoveries of pyrite and galena vary slightly with chitosan (2–3 and 3–6 kDa), yet greatly with chitosan (10 and 100 kDa). In particular, the difference in flotation recovery between pyrite and galena using chitosan (10 kDa) is much greater than that using chitosan (100 kDa). Furthermore, in Figure 4, the arrows point to the optimum molecular weight (10 kDa) and dosage (400 g/t) of chitosan.

At a certain molecular weight of chitosan, recoveries of pyrite and galena decrease gradually with the increase of dosage. Notably, when the chitosan (10 kDa) dosage is increased to 400 g/t, galena recovery drops significantly to 10.29%, whereas the pyrite recovery decreases slightly to 75.02%. Hence, using 400 g/t of chitosan (10 kDa), 1600 g/t of ethyl xanthate, and 100 g/t of terpineol, the maximum recovery difference (64.73%) between pyrite and galena can be achieved. This is the preferred reagent scheme for subsequent experiments.

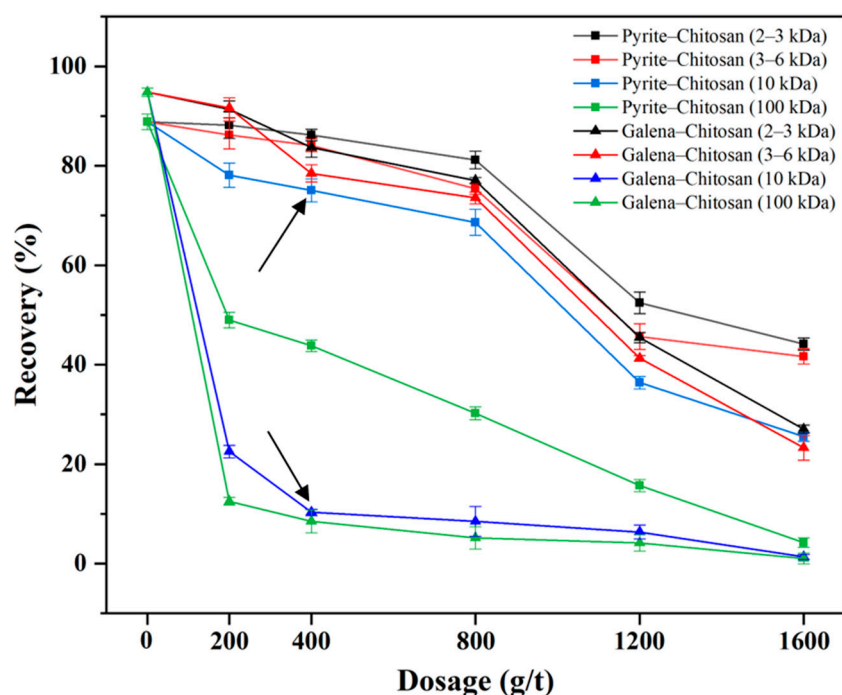


**Figure 4.** Pyrite and galena recovery results of single-mineral flotation experiments using chitosan with different dosages and molecular weights as a depressant, 1600 g/t ethyl xanthate as a collector, and 100 g/t terpeneol as a frother at pH 8.

### 3.2. Mixed-Mineral Flotation Experiments Results

To further evaluate the flotation separation performance of chitosan with different molecular weights, flotation experiments of mixed pyrite/galena minerals were carried out under the preferred reagent scheme (400 g/t of chitosan with different molecular weights, 1600 g/t of ethyl xanthate, and 100 g/t of terpeneol), with the results shown in Table 1.

**Table 1.** The results of mixed-mineral flotation experiments using 400 g/t chitosan with different molecular weights as a depressant, 1600 g/t ethyl xanthate as a collector, and 100 g/t terpeneol as a frother at pH 8.

Chitosan with Different Molecular Weights (kDa)	Flotation Product	Weight (g)	Recovery (%)		Grade (%)	
			Fe	Pb	Fe	Pb
-	Iron concentrate	1.68	81.83	85.72	22.78	44.28
	Lead concentrate	0.32	18.17	14.28	17.22	55.72
2–3	Iron concentrate	1.59	78.91	79.65	22.98	43.11
	Lead concentrate	0.41	21.09	20.35	23.50	42.14
3–6	Iron concentrate	1.49	75.57	73.39	23.43	42.28
	Lead concentrate	0.51	24.43	26.61	22.10	44.74
10	Iron concentrate	0.86	74.04	11.98	39.75	11.95
	Lead concentrate	1.14	25.96	88.02	10.52	66.27
100	Iron concentrate	0.52	40.32	11.54	35.90	19.10
	Lead concentrate	1.48	59.68	88.46	18.60	51.25
-	Mixed minerals	-	-	-	23.09	42.91

Note: The values in parentheses denote deviations.

Table 1 shows that, when using chitosan with a MW of 2–3 kDa, the metal grades in iron concentrates and lead concentrates are comparable (22.98% Fe and 43.11% Pb in iron concentrates, and 23.50% Fe and 42.14% Pb in lead concentrates). Analogously, chitosan with a MW of 3–6 kDa also shows inferior selectivity (23.43% Fe and 42.28% Pb in iron concentrates, and 22.1% Fe and 44.74% Pb in lead concentrates).

These results demonstrate that chitosans with a low molecular weight (2–3 and 3–6 kDa) fail to perform depression selectivity. In contrast, when chitosan (10 and 100 kDa) is used, significant improvements of the Fe grade in iron concentrates and the Pb grade in lead concentrates are obtained. In particular, when chitosan (10 kDa) is used, the Fe grade in iron concentrates and the Pb grade in lead concentrates stand at 39.75% and 66.27%, respectively, which are higher than those of 35.90% and 51.25% when chitosan (100 kDa) is used. In addition, with 400 g/t of chitosan (10 kDa) as a depressant, the maximum recovery difference between Fe and Pb in pyrite or lead concentrates is 62.60%, compared with that of 28.78% with 400 g/t of chitosan (100 kDa).

### 3.3. Zeta Potential Measurements Results

The zeta potential measurement is conducted to reveal the flotation mechanism [42–44]. Zeta potentials of pyrite and galena in the presence or absence of 400 g/t of chitosan with different molecular weights were measured under pH 2–12. As shown in Figure 5, the isoelectric points (IEP) of bare pyrite and galena occurred at about pH 3, which is in line with previous reports [45–47].

As can be seen from Figure 5, compared with zeta potential curves of bare pyrite and galena, the curves of both pyrite and galena with chitosan (2–3 and 3–6 kDa) present a very weak negative shift at pH 4–12. Furthermore, in the presence of chitosan (100 kDa), the zeta potential curves of both pyrite and galena demonstrate a strong negative shift at pH 4–12. However, in the presence of chitosan (10 kDa), the zeta potential curve of galena shows a strong negative shift, while that of pyrite presents a slight one.

At a dosage of 400 g/t and pH 8, and in the presence of chitosan with different molecular weights, the zeta potential changes of pyrite and galena are presented in Table 2. Compared with that of pyrite and galena, the zeta potential values in the presence of chitosan (2–3 and 3–6 kDa) exhibit a slight negative decrease. In addition, in the presence of chitosan (100 kDa), the zeta potential values of pyrite and galena are significantly reduced by 11.3 and 22.2 mV, respectively. However, in the presence of chitosan (10 kDa), the zeta potential value of galena drops greatly by 21.3 mV at pH 8, while that of pyrite exhibits a negligible diminution by 4.0 mV.

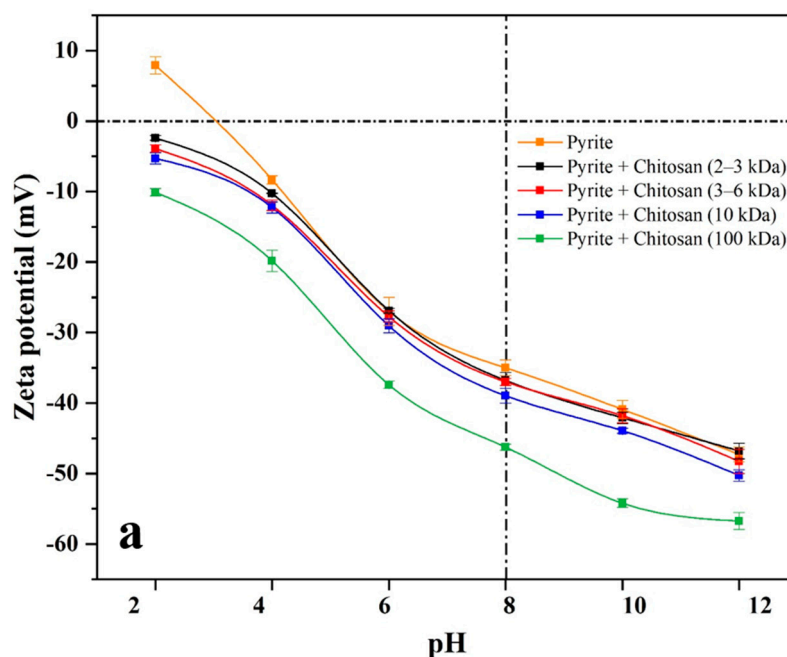
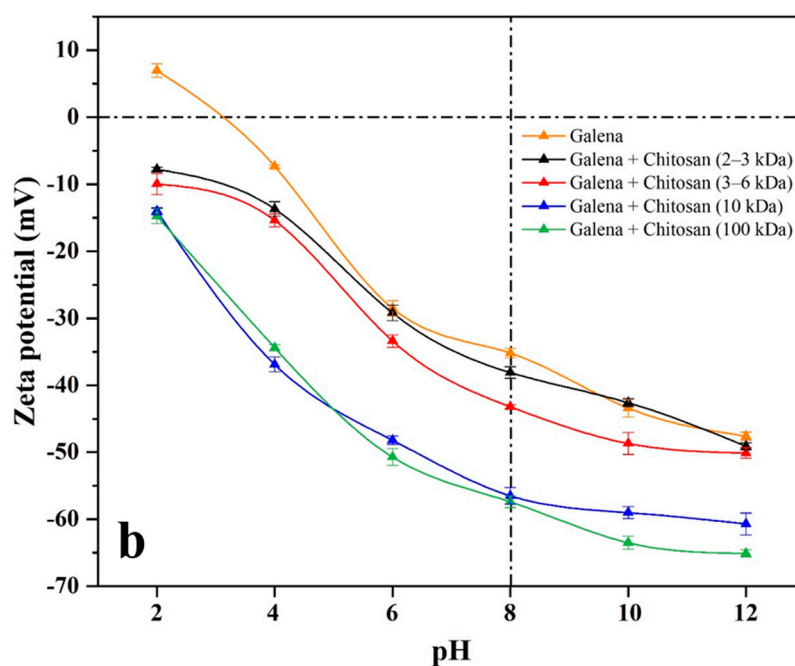


Figure 5. Cont.





**Figure 5.** The effect of the addition of chitosan with different molecular weights (400 g/t) on the zeta potential of (a) pyrite and (b) galena.

**Table 2.** Zeta potential changes (mV) of pyrite and galena in the presence of chitosan with different molecular weights (400 g/t) at pH 8.

System	Chitosan with Different Molecular Weights (kDa)			
	2–3	3–6	10	100
<i>Pyrite + Chitosan</i>	−1.8	−2.0	−4.0	−11.3
<i>Galena + Chitosan</i>	−2.9	−8.0	−21.3	−22.2

### 3.4. Contact Angle Tests Results

Establishing the contact angle is a good method for determining the hydrophobicity of a mineral surface and measuring a mineral's floatability [48–51]. To further explore the mechanism of flotation separation, the contact angles of pyrite and galena surfaces in the presence or absence of chitosan with different molecular weights (400 g/t), at pH 8, were tested. As shown in Figure 6, the contact angle values of pyrite and galena conditioned with DI water stand at 58.8 and 69.3°, respectively. Compared with the results conditioned with DI water, the contact angles of pyrite and galena in the presence of chitosan (2–3 and 3–6 kDa) decrease marginally by 4.5 and 1.7° (chitosan (2–3 kDa)) or 5.7 and 3.4° (chitosan (3–6 kDa)), respectively. The contact angles of pyrite and galena in the presence of chitosan (100 kDa) decrease significantly by 16.1 and 32.1°, respectively. However, in the presence of chitosan (10 kDa), the contact angle of galena reduces sharply by 30.6°, while that of pyrite decreases slightly by 9.5°.

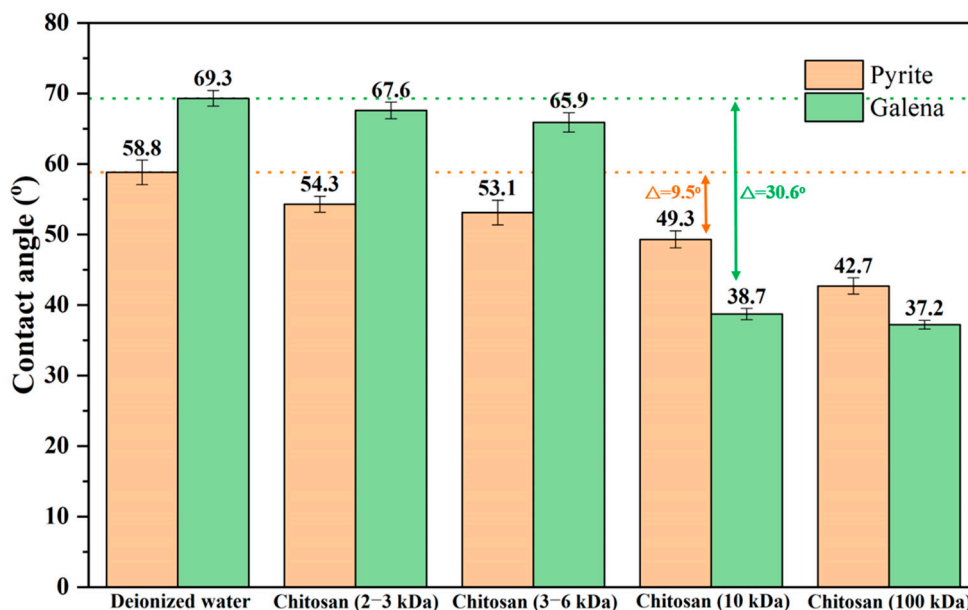


**Figure 6.** The effect of the addition of chitosan with different molecular weights (400 g/t) on the contact angles of (a) pyrite and (b) galena.

#### 4. Discussion

The single-mineral flotation results demonstrated that, under the proposed reagent scheme (400 g/t chitosan with different molecular weights, 1600 g/t of ethyl xanthate, and 100 g/t of terpineol), the depression effect of chitosan could be significantly improved with an increase in molecular weight from 2–3 to 100 kDa [52]. Chitosan (2–3 kDa) and chitosan (3–6 kDa) possess no selective depression effect due to their weak depression abilities for both pyrite and galena. However, both chitosan (10 kDa) and chitosan (100 kDa) have selective depression on galena, and the former has a much better selectivity, which leads to a bigger recovery difference between pyrite and galena. This result means that the separation performance is better by using this reagent scheme. The results of mixed-mineral flotation further confirm that chitosan (2–3 kDa) and chitosan (3–6 kDa) have no separation effect, whereas both chitosan (10 kDa) and chitosan (100 kDa) have a separation effect. The chitosan (100 kDa) obtains a limited separation performance [29,53], while chitosan (10 kDa) has a much better performance, obtaining a high-grade lead concentrate with a Pb grade of 66.27% and a Pb recovery of 88.02% from the feed with a Pb grade of 42.91%. The flotation effect is better than other depressants previously reported [11,12,29].

Huang et al [29]. previously used chitosan to depress pyrite and float galena. In their study, a reagent scheme of  $1.25 \times 10^{-4}$  mol/L of ethyl xanthate (EX), chitosan (100–300 kDa, 75–85% deacetylation), and pH 4 was employed, which is different from the scheme here (e.g.,  $5.5 \times 10^{-4}$  mol/L of EX, chitosan (100 kDa, 85–98% deacetylation), and pH 8). In addition, the samples used for their flotation experiments were sourced differently from those used in this study. It can be concluded that the chitosan with different molecular weights and deacetylation levels at a different pH can lead to distinctly different flotation performances.

The values of the zeta potential and contact angle on the surfaces of both pyrite and galena change slightly in the presence of chitosan (2–3 kDa) or chitosan (3–6 kDa), indicating a weak adsorption and, as a result, a slight depression for both minerals. In the presence of chitosan (100 kDa), the opposite is the case. Therefore, chitosans (2–3, 3–6, and 100 kDa) exhibit no adsorption selectivity on pyrite and galena, and, therefore, the selective separation cannot be achieved. However, in the presence of chitosan (10 kDa) and at pH 8, the zeta potential (21.3 mV) and contact angle ( $30.6^\circ$ ) on the galena surface decrease significantly, while the zeta potential (4.0 mV) and contact angle ( $9.5^\circ$ ) on the pyrite surface only show a slight decrease, indicating that chitosan (10 kDa) is selectively adsorbed



on galena rather than pyrite. Therefore, the preferred reagent scheme (400 g/t of chitosan (10 kDa), 1600 g/t of ethyl xanthate, and 100 g/t of terpineol) can be an effective pyrite-removal strategy to upgrade lead concentrates.

## 5. Conclusions

In this work, the flotation separation performance of chitosan with different molecular weights on pyrite and galena was studied. A novel reagent scheme, i.e., 400 g/t of chitosan (10 kDa) as a depression, 1600 g/t of ethyl xanthate as a collector, and 100 g/t of terpineol as a frother, can achieve the reverse flotation separation of pyrite from galena at pH 8. Zeta potential and contact angle measurements revealed a stronger chitosan (10 kDa) adsorption on the galena surface than on the pyrite surface. Thus, chitosan (10 kDa) has a good industrial application potential to separate pyrite from galena to upgrade lead concentrates.

**Author Contributions:** Methodology, Z.G.; formal analysis, Y.H. and W.S.; investigation, W.Z. and J.C.; Writing—Original-draft preparation, W.Z. and J.C.; Writing—Review and editing, Z.G.

**Funding:** This research was funded by the National Natural Science Foundation of China (51774328 and 51404300), the Young Elite Scientists Sponsorship Program by CAST (2017QNRC001), the Young Elite Scientists Sponsorship Program by Hunan province of China (2018RS3011), the Natural Science Foundation of Hunan Province of China (2018JJ2520), the Open-End Fund for the Valuable and Precision Instruments of Central South University (CSUZC201806), the Open Fund of Guangdong Provincial Key Laboratory of Development and Comprehensive Utilization of Mineral Resources (2017B030314046), and the National 111 Project (B14034).

**Acknowledgments:** The authors would like to thank the editors and the anonymous reviewers for their helpful and constructive comments.

**Conflicts of Interest:** The authors declare no conflict of interest.

## References

1. Cao, Z.; Chen, X.; Peng, Y. The role of sodium sulfide in the flotation of pyrite depressed in chalcopyrite flotation. *Miner. Eng.* **2018**, *119*, 93–98. [\[CrossRef\]](#)
2. Mehrabani, J.V.; Noaparast, M.; Mousavi, S.M.; Dehghan, R.; Rasooli, E.; Hajizadeh, H. Depression of pyrite in the flotation of high pyrite low-grade lead-zinc ore using *Acidithiobacillus ferrooxidans*. *Miner. Eng.* **2010**, *23*, 10–16. [\[CrossRef\]](#)
3. Moslemi, H.; Gharabaghi, M. A review on electrochemical behavior of pyrite in the froth flotation process. *J. Ind. Eng. Chem.* **2017**, *47*, 1–18. [\[CrossRef\]](#)
4. Mu, Y.; Peng, Y.; Lauten, R.A. The depression of pyrite in selective flotation by different reagent systems—A Literature review. *Miner. Eng.* **2016**, *96*, 143–156. [\[CrossRef\]](#)
5. Zhang, C.; Liu, C.; Feng, Q.; Chen, Y. Utilization of N-carboxymethyl chitosan as selective depressants for serpentine on the flotation of pyrite. *Int. J. Miner. Process.* **2017**, *163*, 45–47. [\[CrossRef\]](#)
6. Huang, Z.; Wang, J.; Sun, W.; Hu, Y.; Cao, J.; Gao, Z. Selective flotation of chalcopyrite from pyrite using diphosphonic acid as collector. *Miner. Eng.* **2019**, *140*, 105890. [\[CrossRef\]](#)
7. Boulton, A.; Fornasiero, D.; Ralston, J. Selective depression of pyrite with polyacrylamide polymers. *Int. J. Miner. Process.* **2001**, *61*, 13–22. [\[CrossRef\]](#)
8. Li, Y.; Chen, J.; Kang, D.; Guo, J. Depression of pyrite in alkaline medium and its subsequent activation by copper. *Miner. Eng.* **2012**, *26*, 64–69. [\[CrossRef\]](#)
9. Liu, G.; Zhong, H.; Dai, T. The separation of Cu/Fe sulfide minerals at slightly alkaline conditions by using ethoxycarbonyl thionocarbamates as collectors: Theory and practice. *Miner. Eng.* **2006**, *19*, 1380–1384. [\[CrossRef\]](#)
10. Chen, X.; Peng, Y.; Bradshaw, D. Effect of regrinding conditions on pyrite flotation in the presence of copper ions. *Int. J. Miner. Process.* **2013**, *125*, 129–136. [\[CrossRef\]](#)
11. Peng, Y.; Grano, S.; Fornasiero, D.; Ralston, J. Control of grinding conditions in the flotation of galena and its separation from pyrite. *Int. J. Miner. Process.* **2003**, *70*, 67–82. [\[CrossRef\]](#)
12. Feng, B.; Zhang, W.; Guo, Y.; Wang, T.; Luo, G.; Wang, H.; He, G. The flotation separation of galena and pyrite using serpentine as depressant. *Powder Technol.* **2019**, *342*, 486–490. [\[CrossRef\]](#)

13. Zhang, Y.; Hu, Y.; Sun, N.; Khoso, S.A.; Wang, L.; Sun, W. A novel precipitant for separating lithium from magnesium in high Mg/Li ratio brine. *Hydrometallurgy* **2019**, *187*, 125–133. [\[CrossRef\]](#)
14. McFadzean, B.; Mhlanga, S.S.; O'Connor, C.T. The effect of thiol collector mixtures on the flotation of pyrite and galena. *Miner. Eng.* **2013**, *50*, 121–129. [\[CrossRef\]](#)
15. Chai, W.; Huang, Y.; Peng, W.; Han, G.; Cao, Y.; Liu, J. Enhanced separation of pyrite from high-sulfur bauxite using 2-mercaptobenzimidazole as chelate collector: Flotation optimization and interaction mechanisms. *Miner. Eng.* **2018**, *129*, 93–101. [\[CrossRef\]](#)
16. Lin, S.; Liu, R.; Sun, W.; Hu, Y.; Gao, Z.; Han, H. Pyrogalllic acid: A novel depressant for bismuthinite in Mo–Bi sulfide ore flotation. *Miner. Eng.* **2019**, *131*, 237–240. [\[CrossRef\]](#)
17. Tian, M.; Gao, Z.; Ji, B.; Fan, R.; Liu, R.; Chen, P.; Sun, W.; Hu, Y. Selective Flotation of Cassiterite from Calcite with Salicylhydroxamic Acid Collector and Carboxymethyl Cellulose Depressant. *Minerals* **2018**, *8*, 316. [\[CrossRef\]](#)
18. Yin, Z.; Sun, W.; Hu, Y.; Zhang, C.; Guan, Q.; Zhang, C. Separation of Molybdenite from Chalcopyrite in the Presence of Novel Depressant 4-Amino-3-thioxo-3,4-dihydro-1,2,4-triazin-5(2H)-one. *Minerals* **2017**, *7*, 146. [\[CrossRef\]](#)
19. Gao, Z.; Gao, Y.; Zhu, Y.; Hu, Y.; Sun, W. Selective flotation of calcite from fluorite: A novel reagent schedule. *Minerals* **2016**, *6*, 114. [\[CrossRef\]](#)
20. Wang, J.; Zhou, Z.; Gao, Y.; Sun, W.; Hu, Y.; Gao, Z. Reverse Flotation Separation of Fluorite from Calcite: A Novel Reagent Scheme. *Minerals* **2018**, *8*, 313. [\[CrossRef\]](#)
21. Ahmadi, M.; Gharabaghi, M.; Abdollahi, H. Effects of type and dosages of organic depressants on pyrite floatability in microflotation system. *Adv. Powder Technol.* **2018**, *29*, 3155–3162. [\[CrossRef\]](#)
22. Bulatovic, S.M. Use of organic polymers in the flotation of polymetallic ores: A review. *Miner. Eng.* **1999**, *12*, 341–354. [\[CrossRef\]](#)
23. Duarte, R.S.; Lima, R.M.F.; Leão, V.A. Effect of inorganic and organic depressants on the cationic flotation and surface charge of rhodonite-rhodochrosite. *Rem. Rev. Esc. Minas* **2015**, *68*, 463–469. [\[CrossRef\]](#)
24. Sarquís, P.E.; Menéndez-Aguado, J.M.; Mahamud, M.M.; Dzioba, R. Tannins: The organic depressants alternative in selective flotation of sulfides. *J. Clean. Prod.* **2014**, *84*, 723–726. [\[CrossRef\]](#)
25. Guo, Q.; Feng, B.; Zhang, D.; Guo, J. Flotation separation of chalcopyrite from talc using carboxymethyl chitosan as depressant. *Physicochem. Probl. Miner. Process.* **2017**, *53*, 1255–1263. [\[CrossRef\]](#)
26. Wang, K.; Liu, Q. Adsorption of phosphorylated chitosan on mineral surfaces. *Colloids Surf. A Physicochem. Eng. Aspects* **2013**, *436*, 656–663. [\[CrossRef\]](#)
27. Zhang, X.; Zhu, Y.; Zheng, G.; Han, L.; McFadzean, B.; Qian, Z.; Piao, Y.; O'Connor, C. An investigation into the selective separation and adsorption mechanism of a macromolecular depressant in the galena-chalcopyrite system. *Miner. Eng.* **2019**, *134*, 291–299. [\[CrossRef\]](#)
28. McFadzean, B.; Dicks, P.; Groenmeyer, G.; Harris, P.; O'Connor, C. The effect of molecular weight on the adsorption and efficacy of polysaccharide depressants. *Miner. Eng.* **2011**, *24*, 463–469. [\[CrossRef\]](#)
29. Huang, P.; Cao, M.; Liu, Q. Selective depression of pyrite with chitosan in Pb–Fe sulfide flotation. *Miner. Eng.* **2013**, *46*, 45–51. [\[CrossRef\]](#)
30. Garcia Vidal, C.A.; Pawlik, M. Molecular weight effects in interactions of guar gum with talc. *Int. J. Miner. Process.* **2015**, *138*, 38–43. [\[CrossRef\]](#)
31. Liu, C.; Feng, Q.; Shi, Q.; Zhang, W.; Song, S. Utilization of N-carboxymethyl chitosan as a selective depressant for talc in flotation of chalcopyrite. *Physicochem. Probl. Miner. Process.* **2019**, *55*, 108–115. [\[CrossRef\]](#)
32. Hu, Y.; Gao, Z.; Sun, W.; Liu, X. Anisotropic surface energies and adsorption behaviors of scheelite crystal. *Colloids Surf. A Physicochem. Eng. Aspects* **2012**, *415*, 439–448. [\[CrossRef\]](#)
33. Porento, M.; Hirva, P. Theoretical studies on the interaction of anionic collectors with  $\text{Cu}^+$ ,  $\text{Cu}^{2+}$ ,  $\text{Zn}^{2+}$  and  $\text{Pb}^{2+}$  ions. *Theor. Chem. Acc.* **2002**, *107*, 200–205. [\[CrossRef\]](#)
34. Huangfu, Z.; Khoso, S.A.; Sun, W.; Hu, Y.; Chen, C.; Zhang, Q. Utilization of petrochemical by-products as a new frother in flotation separation of molybdenum. *J. Clean. Prod.* **2018**, *204*, 501–510. [\[CrossRef\]](#)
35. Gao, Y.; Gao, Z.; Sun, W.; Hu, Y. Selective flotation of scheelite from calcite: A novel reagent scheme. *Int. J. Miner. Process.* **2016**, *154*, 10–15. [\[CrossRef\]](#)
36. Gao, Y.; Gao, Z.; Sun, W.; Yin, Z.; Wang, J.; Hu, Y. Adsorption of a novel reagent scheme on scheelite and calcite causing an effective flotation separation. *J. Colloid Interface Sci.* **2018**, *512*, 39–46. [\[CrossRef\]](#)

37. Li, C.; Gao, Z. Effect of grinding media on the surface property and flotation behavior of scheelite particles. *Powder Technol.* **2017**, *322*, 386–392. [\[CrossRef\]](#)
38. Tian, M.; Gao, Z.; Han, H.; Sun, W.; Hu, Y. Improved flotation separation of cassiterite from calcite using a mixture of lead (II) ion/benzohydroxamic acid as collector and carboxymethyl cellulose as depressant. *Miner. Eng.* **2017**, *113*, 68–70. [\[CrossRef\]](#)
39. Fuerstenau, D.W. Pradip Zeta potentials in the flotation of oxide and silicate minerals. *Adv. Colloid Interface Sci.* **2005**, *114*, 9–26. [\[CrossRef\]](#)
40. Niu, X.; Ruan, R.; Xia, L.; Li, L.; Sun, H.; Jia, Y.; Tan, Q. Correlation of surface adsorption and oxidation with a floatability difference of galena and pyrite in high-alkaline lime systems. *Langmuir* **2018**, *34*, 2716–2724. [\[CrossRef\]](#)
41. Chau, T.T. A review of techniques for measurement of contact angles and their applicability on mineral surfaces. *Miner. Eng.* **2009**, *22*, 213–219. [\[CrossRef\]](#)
42. Gao, Z.; Hu, Y.; Sun, W.; Drelich, J.W. Surface-Charge Anisotropy of Scheelite Crystals. *Langmuir* **2016**, *32*, 6282–6288. [\[CrossRef\]](#)
43. Jiang, W.; Gao, Z.; Khoso, S.A.; Gao, J.; Sun, W.; Pu, W.; Hu, Y. Selective adsorption of benzhydroxamic acid on fluorite rendering selective separation of fluorite/calcite. *Appl. Surf. Sci.* **2018**, *435*, 752–758. [\[CrossRef\]](#)
44. Wang, J.; Gao, Z.; Gao, Y.; Hu, Y.; Sun, W. Flotation separation of scheelite from calcite using mixed cationic/anionic collectors. *Miner. Eng.* **2016**, *98*, 261–263. [\[CrossRef\]](#)
45. Feng, B.; Lu, Y.; Luo, X. The effect of quartz on the flotation of pyrite depressed by serpentine. *J. Mater. Res. Technol.* **2015**, *4*, 8–13. [\[CrossRef\]](#)
46. Mitchell, T.K.; Nguyen, A.V.; Evans, G.M. Heterocoagulation of chalcopyrite and pyrite minerals in flotation separation. *Adv. Colloid Interface Sci.* **2005**, *114*, 227–237. [\[CrossRef\]](#)
47. Santhiya, D.; Subramanian, S.; Rao, K.H.; Natarajan, K.A.; Forssberg, K.S.E. Bio-modulation of galena and sphalerite surfaces using thiobacillus thiooxidans. *Int. J. Miner. Process.* **2001**, *62*, 121–141. [\[CrossRef\]](#)
48. Gao, Z.; Fan, R.; Ralston, J.; Sun, W.; Hu, Y. Surface broken bonds: An efficient way to assess the surface behaviour of fluorite. *Miner. Eng.* **2019**, *130*, 15–23. [\[CrossRef\]](#)
49. Gao, Z.; Xie, L.; Cui, X.; Hu, Y.; Sun, W.; Zeng, H. Probing Anisotropic Surface Properties and Surface Forces of Fluorite Crystals. *Langmuir* **2018**, *34*, 2511–2521. [\[CrossRef\]](#)
50. Guo, H.; Yen, W. Surface potential and wettability of enargite in potassium amyl xanthate solution. *Miner. Eng.* **2002**, *15*, 405–414. [\[CrossRef\]](#)
51. Yekeler, M.; Ulusoy, U.; Hiçyılmaz, C. Effect of particle shape and roughness of talc mineral ground by different mills on the wettability and floatability. *Powder Technol.* **2004**, *140*, 68–78. [\[CrossRef\]](#)
52. Bicak, O.; Ekmekci, Z.; Bradshaw, D.J.; Harris, P.J. Adsorption of guar gum and CMC on pyrite. *Miner. Eng.* **2007**, *20*, 996–1002. [\[CrossRef\]](#)
53. Huang, P.; Cao, M.; Liu, Q. Using chitosan as a selective depressant in the differential flotation of Cu-Pb sulfides. *Int. J. Miner. Process.* **2012**, *106*, 8–15. [\[CrossRef\]](#)

